Handheld Analyzer with On-Chip Molecularly-Imprinted Biosensors for Electrical Detection of Propofol in Plasma Samples

Chien-Chong Hong, Chih-Chung Lin, Chian-Lang Hong, Zi-Xiang Lin, Meng-Hua Chung, Pei-Wen Hsieh

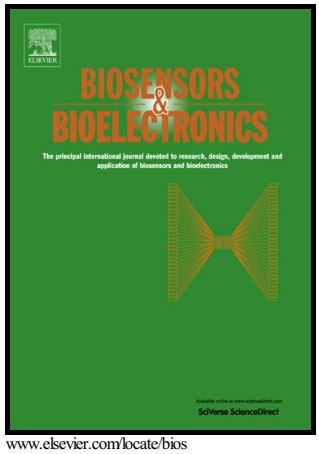

www.elsevier.com/locate/bios

PII: S0956-5663(16)30661-3
DOI: http://dx.doi.org/10.1016/j.bios.2016.07.032
Reference: BIOS8913

To appear in: *Biosensors and Bioelectronic*

Received date: 10 May 2016
Revised date: 29 June 2016
Accepted date: 9 July 2016

Cite this article as: Chien-Chong Hong, Chih-Chung Lin, Chian-Lang Hong, Zi Xiang Lin, Meng-Hua Chung and Pei-Wen Hsieh, Handheld Analyzer with On Chip Molecularly-Imprinted Biosensors for Electrical Detection of Propofol i Plasma Samples, *Biosensors and Bioelectronic* http://dx.doi.org/10.1016/j.bios.2016.07.032

Handheld Analyzer with On-Chip Molecularly-Imprinted Biosensors for Electrical Detection of Propofol in Plasma Samples

Chien-Chong Hong[1*], Chih-Chung Lin[2], Chian-Lang Hong[3,4*],

Zi-Xiang Lin[1], Meng-Hua Chung[1], Pei-Wen Hsieh[2,5]

[1]*BioMEMS and Nanobiosystems Laboratory*, Department of Power Mechanical Engineering, National Tsing Hua University, Hsinchu, Taiwan

[2]Department of Anesthesiology, Chang Gung Memorial Hospital, Taoyuan, Taiwan

[3]Department of Anesthesiology, Chang Gung Memorial Hospital, Chiayi, Taiwan

[4]Chang Gung University of Science and Technology, Chiayi, Taiwan

[5]Graduate Institute of Natural Products, School of Traditional Chinese Medicine, and Graduate Institute of Biomedical Sciences, College of Medicine, Chang Gung University, Taoyuan, Taiwan

Corresponding authors:

Chien-Chong Hong, Tel: 886-3-5715131ext.33736, Fax: 886-3-5722840, email: chong@pme.nthu.edu.tw, address: 101, Sec. 2, Kung Fu Rd., Engineering Building I, Rm. 629, Hsinchu, Taiwan

Chian-Lang Hong, Tel: 886-5-3621000 ext.2525, Fax: 886-5-3623002, email: leisure@cgmh.org.tw, address: 6.West Sec. Chia Pu Road, Putzu City, ChiaYi Hsien, Taiwan

ABSTRACT

This paper proposes a novel handheld analyzer with disposable lab-on-a-chip technology

for the electrical detection of the anesthetic propofol in human plasma samples for clinical diagnoses. The developed on-chip biosensors are based on the conduction of molecularly imprinted polymers (MIPs) that employ label-free electrical detection techniques. Propofol in total intravenous anesthesia is widely used with a target-controlled infusion system. At present, the methods employed for detecting blood propofol concentrations in hospitals comprise high-performance liquid chromatography and ion mobility spectrometry. These conventional instruments are bulky, expensive, and difficult to access. In this study, we developed a novel plastic microfluidic biochip with an on-chip anesthetic biosensor that was characterized for the rapid detection of propofol concentrations. The experimental results revealed that the response time of the developed propofol biosensors was 25 s. The specific binding of an MIP to a nonimprinted polymer (NIP) reached up to 560%. Moreover, the detection limit of the biosensors was 0.1 μg/mL, with a linear detection range of 0.1 to 30 μg/mL. The proposed disposable microfluidic biochip with an on-chip anesthetic biosensor using MIPs exhibited excellent performance in the separation and sensing of propofol molecules in the human plasma samples. Compared with large-scale conventional instruments, the developed microfluidic biochips with on-chip MIP biosensors present the advantages of a compact size, high selectivity, low cost, rapid response, and single-step detection.

Keywords: propofol, microfluidic chip, molecularly imprinted polymer, biosensor, label-free electrical detection

1. INTRODUCTION

The intravenous anesthetic agent propofol (2.6-diisopropylphenol) is a short-acting general anesthetic that is widely used for induction and maintenance through continuous IV infusion and rapid recovery in clinical practice. In total intravenous anesthesia, propofol has recently become a popular and practical anesthetic because of the availability of a propofol target-controlled infusion (TCI) pump with a built-in TCI system, which enables the user to set the propofol injection concentration by using computer-controlled pharmacokinetic models (e.g., the Marsh model and the Schnider model). However, patient pharmacokinetics and pharmacodynamics vary with age, cardiac output, coexisting diseases, concurrent drug administration, body temperature, and bodyweight (Coetzee et al., 1995). These factors play a critical role in determining target concentrations of propofol. Propofol has sedative and hypnotic effects, and the anesthetic depth is determined for the effect site in brain. However, it is infeasible in clinical practice to determine the propofol concentration in the brain. Even if we could directly measure the concentration of propofol in the brain, it would be necessary to know the accurate propofol concentrations in the plasma. Currently, a method for measuring or detecting the real-time anesthetic propofol agent concentration, confirming that the drug has reached the effect site, is unavailable.

Several methods are used for monitoring the depth of anesthesia, including monitoring the bispectral index, which reflects a signal-processed electroencephalographic parameter (Ouchi, 2015). However, at present, an ideal, highly reliable monitor is unavailable. In one study, the electroencephalography patterns showed high variation during propofol treatment (Sigalovsky, 2003). Patient awareness under general anesthesia remains unpreventable (Khan et al., 2014). Several studies have reported abnormal blood propofol concentrations during infusion

in obese patients (Tachibana et al., 2014) and epidural blockade-dosed patients (Sitsen et al., 2016), as well as hypothermia effects in intensive care unit patients (Bjelland et al., 2013) and scoliosis-operated children (Panchatsharam et al., 2014). Numerous past studies have compared their results in using various traditional instruments for the detection of plasma propofol concentrations, such as high-performance liquid chromatography and ion mobility spectrometry (Yarbrough et al., 2012; Zhou et al., 2015). These conventional instruments are bulky, expensive, and difficult to access. In addition, only people who have received proper training can operate them; furthermore, these instruments cannot be used to detect real-time propofol concentrations in human plasma samples. To achieve effective blood propofol concentrations and avoid adverse effects resulting from excessive or insufficient propofol administration, we require a more convenient clinical means of monitoring blood propofol concentrations.

Certain studies have investigated the possibility of propofol sensing for breath gases (Harrison et al., 2003; Laurila et al., 2011). It's unclear understanding to relate blood concentrations in breath samples. Past studies have investigated propofol-sensing on the basis of optical detection with molecularly imprinted polymers (MIPs) (Hong, et al., 2010; Li et al., 2012), optical detection with solid phase extraction (Cowley et al., 2012) and electrochemical detection with PVC membrane-coated sensors (Kivlehan et al., 2015).

The demand for point-of-care testing in clinical diagnostics is increasing. Point-of-care assays can considerably improve the quality of medical care. In the past decade, technologies for clinical diagnostics have been widely developed and successfully applied in several fields (Abel, 2015). Among these technologies, in which lab-on-a-chip applications and microfluidics play a critical role (Chin et al., 2007; Mohammed et al., 2011), it is most crucial to achieve biosensors with highly specific recognition and highly sensitive transduction. Molecular imprinting provides

an approach to highly specific binding that has been adapted from biological antigen and antibody binding. The molecular imprinting method is relatively simple and easy to perform in a suitable fashion, requiring only functional monomers, templates, solvents, and cross-linking agents. In molecular imprinting, polymerization is followed by the removal of the template. During these processes, a number of functional monomers are assembled in an orderly manner, with their functional groups placed at the desired sites within cavities of the desired size. Therefore, MIPs with binding sites, having a specific shape and functional group recognition, can be used for performing high-specificity and high-selectivity sensing on the target molecular compound (Uzun and Turner, 2016). A morphological study of nanocavities on MIPs reported an enhancement in MIP performance (Hong et al., 2012). MIP materials have exhibited good performance in separating or extracting target proteins from blood plasma samples (Hong et al., 2013; Karimian et al., 2013; Chen et al., 2016; Gao et al., 2015). In another study, MIPs were realized on ITO electrodes for electrochemical sensing (Yoshimi et al., 2013).

Conducting polymers are widely used in gas and chemical sensors (Janata and Josowicz, 2003). Pyrrole is the most extensively employed conducting polymer in electrochemical biosensors (Ramanavicius et al., 2006). Furthermore, certain studies have applied conducting MIPs on Au and Pt electrodes for electrochemical sensing (Lakshmi et al., 2009; Ramanaviciene and Ramanavicius, 2004). Because of the considerably smaller impedance, conducting MIPs have higher sensitivity with electrical or electrochemical detection compared with nonconducting MIPs. The challenge presented by nonconductive MIPs in electrical biosensors can be addressed by conducting a precise, thin conformal deposition (approximately 10 nm) of nonconducting MIPs on nanotubes to enhance the performance of electrical MIP biosensors (Cai et al., 2010).

In a past study, we devised microfluidic biochips with on-chip MIP films on the basis of the colorimetric principle, with Gibb's reagent for propofol detection (Hong et al., 2010). Compared with the optical sensing mechanism, electrical sensing provides a more effective and direct approach with compact structures for the transduction of analyte recognition. In addition, electrical sensing can easily be directly integrated with handheld, embedded electronic systems. Furthermore, label-free detection, which does not require color reagents or label tags, can be applied during electrical detection with conducting MIPs. In this study, we developed and characterized a handheld analyzer with molecularly imprinted biosensors for electrical detection of anesthetic propofol in plasma samples. An alternative simplified detection method is used for a cost-effective handheld analyzer. The proposed analyzer presents the following advantages: compact design, full integration, ease of use, high specificity, cost effectiveness, rapid response, small sample volume, and single-step detection.

<Scheme 1>

2. MATERIALS AND METHODS

The electrical propofol detection system includes a handheld analyzer and a disposable plastic lab on a chip with conducting molecularly imprinted biosensors. As shown in Scheme 1a, the handheld platform consists of Java-programmed controlled ARM-11-based embedded systems, a 4-inch touchscreen, charging and discharging circuit, battery, electronic chip socket, and disposable microfluidic biochip with on-chip biosensors. The general-purpose input and output (GPIO) interface on the embedded board is used to trigger the charging and discharging circuit. The analog-to-digital (ADC) module on the embedded board is employed for signal data

acquisition from the biosensors to the embedded system for further data processing. Scheme 1b shows a schematic of the microfluidic biochips with on-chip molecularly imprinted biosensors for propofol sensing; the microfluidic biochip was designed for the precise transport of samples to the biosensor microchambers by capillary force. The microfluidic chip has a three-layer structure. The fluidic inlets and outlets are on the top layer. Patterned double-sided stickers are positioned between the top and bottom layers to form a microfluidic channel. In addition, the conducting MIP electrical biosensors are situated on the bottom layer. Compared to non-conducting MIP electrodes, conducting MIP electrodes have much lower impedance, which are higher sensitivity and better accuracy in tiny surface change. The imprinted nanocavities on the MIPs are used for the specific binding of propofol molecules. The working principle of the molecularly imprinted biosensors is depicted in Scheme 1c. When propofol molecules are separated from human plasma samples and captured by MIP biosensors, the surface electrical properties on the MIP biosensors are altered because of the binding of the propofol molecules, which reduces the conductivity of the MIPs. The biosensors are used to directly detect electrical changes. The binding of propofol molecules on the MIPs affects the time constant of the discharging curves. The conducting MIP, which provides highly specific binding to the analyte, is used for separating and sensing propofol, functioning as a plastic antibody for capturing propofol in human plasma samples.

The electrical equivalent circuits of the conducting MIP IDA biosensor in the microfluidic channel are shown in Scheme 2a. C_{cp} and R_{cp} represent the surface capacitance and resistance of the biosensor, respectively. The electrical equivalent circuits of a single conducting MIP before and after propofol molecular binding are shown in Scheme 2b. Propofol is a nonconducting molecule; after analyte binding on MIPs, propofol molecules in imprinted

nanocavities contribute surface capacitance and also block some conductivity of MIPs, thereby increasing surface impedance. The changes in surface impedance could be measured by a costly LCR meter. However, to realize propofol sensing with a cost-effective handheld analyzer, the discharging detection mechanism was employed to measure the propofol concentration, rather than measuring the surface impedance directly. The time constant, which was derived from the discharging curve of the MIP biosensor, was used to sense changes in surface impedance.

<Scheme 2>

For this study, pyrrole and propofol were purchased from Sigma-Aldrich for the electropolymerization process. Cyclic olefin copolymers (COCs) (Topas COC 6015, Tg: 150ºC) were chosen as the chip substrates. Because COCs exhibit high resistance against several chemical solvents, they are compatible with most processes in biomedical microelectromechanical systems.

3. FABRICATION AND INTEGRATION

The fabrication steps comprised the fabrication of the microfluidic biochips and the MIP biosensors as well as the encapsulation of the device. A plastic material, namely COC, was chosen as the substrate. In this study, 4-inch COC wafers with a thickness of 1.4 mm were fabricated using plastic injection molding techniques, and MIP biosensors were fabricated on the COC substrate. The fabrication process for the MIP membranes involved three steps: combination, electropolymerization, and extraction. A monomer, namely pyrrole, was mixed with template molecules in a methanol solvent. Furthermore, the MIP was composed of

propofol–pyrrole, with a molar ratio of 1:5. A blank 4-inch COC plastic wafer was prepared for electron beam deposition of a 100-nm gold film. Photolithography was conducted to pattern four biochips on each COC wafer and four IDA electrodes on each COC biochip. Subsequently, the biochips were immersed in the MIP solution. A LabVIEW-controlled program with power sources was connected to the electrodes. A current density of 25 $\mu A/mm^2$ was applied for 30 s for electropolymerization at 25°C. After the electropolymerization of the conducting polymer electrodes, the imprinted sites were formed by releasing the template molecules from the MIP electrodes with the methanol solvent for 24 h. Then, the MIP film was patterned on gold IDA electrodes. Figure 1a shows the microfluidic stickers, which were composed by pressing a CNC-machined knife mold on 120-μm-thick double-sided tape. The microfluidic channel was formed by sandwich-bonding the patterned double-sided stickers between two blank COC chips. Afterward, the MIP biosensor was integrated with a plastic microfluidic chamber. Figure 1b displays the handheld analyzer with the fabricated COC plastic microfluidic chip. The fabricated plastic microfluidic chip and the on-chip IDA conducting MIP biosensor are shown in Figure 1c and 1d, respectively.

<Figure 1>

4. RESULTS AND DISCUSSION

Figures 2a–2d present the SEM cross-sectional images of the fabricated MIP for various polymerization durations. The thickness of the MIP increased linearly with the duration of polymerization, as shown in Figure 2e. The MIP thickness ranged from 133 to 739 nm. According to the SEM observations, the polymer film had a slightly nonuniform surface

formation for a short deposition duration. In this study, polymerization was set for 30 s to fabricate the MIP. Compared with the optically-polymerized MIP film (Hong et al., 2012), the electropolymerized MIP film had an uneven surface morphology, as shown in Figure S1.

This study was approved by the institutional ethics committee of Chang Gung Memorial Hospital. Written informed consent was obtained from patients undergoing elective surgery. Propofol-free blood samples were obtained before the surgery and were centrifuged for 20 min for plasma separation. The measurements indicated that patient A had139.5 mEg/L of Na^+, 106.7 mEq/L of Cl^-, and 4.62 g/dL of albumin. By contrast, patient B had 134.6 mEg/L of Na^+, 107.7 mEq/L of Cl^-, and 3.00 g/dL of albumin. The plasma sample from patient A was used to establish a calibration curve, and that from patient B was employed for comparison. In the experiment, 2% propofol injection samples were spiked into the plasma samples to obtain samples with different propofol concentrations. The microfluidic chip was inserted into the socket on the battery-powered handheld analyzer for detection. Then, 4-μL plasma samples with known propofol concentrations were dropped at the inlet of the microfluidic biochips. The plasma samples required approximately 6 to 8 s to self-fill the microchannels by capillary force. Afterward, the detection procedure was performed by manipulating the developed Java program in the ARM-embedded system to communicate through the GPIO and ADC interface for discharging trigger, signal processing, data acquisition, and storage. Figure 3 shows the dynamic propofol binding results obtained with an electrochemical impedance spectroscope. From the binding curve for capacitance measurements obtained using an electrical impedance measurement instrument, the binding reached saturation at 20.6 s. After the analyte binding, the capacitance decreased around 28% and the resistance increased around 16%.

<Figure 2>

<Figure 3>

Propofol molecules, which are nonconducting, mainly contribute to changes in surface impedance after binding to the MIP. According to the equivalent circuit of the biosensors, the analyte concentration can be measured by detecting changes in surface impedance, which is related to the captured analyte. The discharging detection mechanism was employed to measure the propofol concentration, rather than measuring the surface impedance directly. The time constant, which was derived from the discharging curve of the MIP biosensor, was used to sense changes in surface impedance. The voltage bias of the biosensor is set to 0.30 V. The developed biosensor began the measurement at 20.6 s. The discharging for 5 seconds is enough for calculating the time constant. According to the measured discharging curves for the NIP and MIP, shown respectively in Figures 4a and 4b, the specific binding of the biosensor reached up to 560%. Figure 4b shows the discharging curves under various propofol concentrations that were measured between 0 and 30 μg/mL. Afterward, the time constants of the discharging curves for the various propofol concentrations could be calculated from the curves. In this study, we tested the discharging curve of the bare gold IDA electrodes in the blood plasma samples with a propofol concentration of 20 μg/mL, finding a slight increase in voltage, as shown in Figure S2. The discharging slopes were calculated as a calibration curve (Figure 4c). The variations of the developed biosensors were tested with different propofol concentrations (Figure 4d). The coefficient of the variations for the propofol biosensors was 6.87%. The proposed electronic

propofol biosensors with MIP electrodes for the electrical detection of propofol exhibited high performance in separating and sensing anesthetic propofol molecules.

The new-generation propofol analyzer is based on the label-free electrical detection method with a conducting MIP. We measured the propofol concentrations of patient B and compared the results by performing HPLC, as shown in Figure S3a. The relative standard deviation was 4.2. Although HPLC cannot be used for determining precise propofol concentrations likely caused by the difficulties of performing column separation with propofol, the results revealed a linear trend. Figure S3b shows the measured propofol concentrations in the plasma sample of patient B that were determined using the developed biosensors on the handheld analyzer; these concentrations were calculated using the calibration curve shown in Figure 4c. The relative standard deviation was 3.3.

In this study, the response time of the developed biosensors was 25 s. The specific binding tests were performed using the characterization of the absorption ratio of propofol molecules on the MIP and NIP surfaces. The specificity (i.e., imprinting factor) of the MIP films was 560%. Because of its high specificity, we believe that the biosensor can be employed for accurate, real-time detection of propofol concentration; furthermore, the biosensor can aid in monitoring the anesthetic level and the pharmacokinetics of propofol under general anesthesia in the future.

<Figure 4>

When whole blood testing is performed, materials (e.g., blood cells) that affect surface electrical properties should be filtered out. Centrifugal plasma separation from whole blood is

currently performed in hospital laboratories. The developed electrical biosensors with on-chip microfilters, in addition to a vacuum module for plasma separation from whole blood—both of which are under investigation—would further simplify the detection process for on-site and point-of-care testing.

5. CONCLUSIONS

In this study, we successfully developed a novel plastic microfluidic biochip with an on-chip anesthetic biosensor that was characterized for the electrical detection of propofol in human plasma samples. The handheld analyzer with on-chip molecularly imprinted biosensors using label-free electrical detection methods demonstrated excellent performance in separating and sensing anesthetic propofol molecules. The experimental findings show that the developed microfluidic system with propofol MIP biosensors can successfully detect propofol samples with concentrations of 0.1 to 30 μg/mL, whereas the specific binding of an MIP was found to reach up to 560%. The limit of detection and the response time of the developed biosensors were 0.1 μg/mL and 25 s, respectively. Compared with conventional large-scale instruments, the developed microfluidic system with MIP biosensors presented the advantages of a compact design, full integration, ease of use, high specificity, cost effectiveness, rapid response, small sample volume, and single-step detection. In the future, the developed label-free electrical biosensors with MIP recognition technique can be further applied in disposable lab-on-chip applications, such as point-of-care protein analysis and on-site food safety analysis, which are under investigation.

ACKNOWLEDGEMENT

This research was supported by the National Science Council of Taiwan (MOST 102-2221-E-007-013-MY2) and Chang Gung Memorial Hospital-National Tsing Hua University Joint Research Project (CMRPG390131 & CMRPG3A0051).

REFERENCES

Abel, G., 2015. Expert Review of Molecular Diagnostics 15(7), 853-855.

Bjelland, T. W., Klepstad, P., Haugen, B. O., Nilsen, T., Dale, O., 2013. Drug Metabolism and Disposition 41, 214-223.

Cai, D., Ren, L., Zhao, H., Xu, C., Zhang, L., Yu, Y., Wang, H., Lan, Y., Roberts, M.F., Chuang, J.H., Naughton, M.J., Ren, Z., Chiles, T.C., 2010. Nature Nanotechnology 5, 597-601.

Chen, F., Zhao, W., Zhang, J., Kong, J., 2016. Physical Chemistry Chemical Physics 18, 718-725.

Chin, C.D., Linder, V., Sia, S.K., 2007. Lab on a Chip 7(41), 41-57.

Coetzee, J. F., Glen, J. B., Wium, C. A., Boshoff, L., 1995. Anesthesiology 82, 1328-45.

Cowley, N. J., Laitenberger, P., Liu, B., Jarvis, J., Clutton-Brock, T. H., 2012. Anaesthesia 67, 870-874.

Gao, R., Zhao, S., Hao, Y., Zhang, L., Cui, X., Liu, D., Zhang, M., Tang, Y., 2015. Journal of Separation Science 38, 3914-3920.

Harrison, G.R., Critchley, A.D.J., Mayhew, C.A., 2003. British Journal of Anaesthesia 91(6), 797-799.

Hong, C.-C., Chang, P.-H., Lin, C.-C., Hong, C.-L., 2010. Biosensors and Bioelectronics 25, 2058-2064.

Hong, C.-C., Lin, C.-C., Hong, C.-L., Chang, P.-H., 2012. Biomedical Microdevices 14(3), 435-441.

Hong, C.-C., Chen, C.-P., Horng, J.-C., Chen, S.-Y., 2013. Biosensors and Bioelectronics 50,

425-430.

Janata, J., Josowicz, M., 2003. Nature Materials 2, 19-24.

Karimian, N., Vagin, M., Zavar, M.H.A., Chamsaz, M., Turner, A.P.F., Tiwari, A., 2013. Biosensors and Bioelectronics 50, 492-498.

Khan, M.S., Zetterlund, E.-L., Green, H., Oscarsson, A., Zackrisson, A.-L., Svanborg, E., Lindholm, M.-L., Persson, H., Eintrei, C., 2014. Basic and Clinical Pharmacology and Toxicology 115, 565-570.

Kivlehan, F., Chaum, E., Lindner, E., 2015. Analyst 140, 98.

Laurila, T., Sorvajarvi, T., Saarela, J., Toivonen, J., Wheeler, D. W., Ciaffoni, L., Ritchie, G.A.D., Kaminski, C.F., 2011. Analytical Chemistry 83, 3963-3967.

Lakshmi, D., Bossi, A., Whitcombe, M.J., Chianella, I., Fowler, S.A., Subrahmanyam, S., Piletska, E.V., Piletsky, S.A., 2009. Analytical Chemistry 81, 3576-3584.

Li, L., Ding, H., Di, B., Li, W., Chen, J., 2012. Analyst 137, 5632.

Mohammed, M.-I., Desmulliez, M.P.Y., 2011. Lab on a Chip 11, 569-595.

Ouchi, K., 2015. Global Journal of Anesthesiol 2(2), 054-056.

Panchatsharam, S., Callaghan, M., Day, R., Sury, M. R. J., 2014. Anesthesia and Analgesia 119, 1150-1157.

Ramanavicius, A., Ramanaviciene, A., Malinauskas, A., 2006. Electrochimica Acta 51, 6025-6037.

Ramanaviciene, A., Ramanavicius, A., 2004. Biosensors and Bioelectronics 20, 1076-1082.

Sigalovsky, N., 2003. AANA Journal 71(5), 373-379.

Sitsen, E., Olofsen, E., Lesman, A., Dahan, A., Vuyk, J., 2016. Anesthesia and Analgesia 122(5), 1341-1349.

Tachibana, N., Niiyama, Y., Yamakage, M., 2014. Eur J. Anaesthesiol 31, 701-707.

Yarbrough, J., Harvey, R., Cox, S., 2012. Journal of Chromatographic Science 50, 162-166.

Yoshimi, Y., Sato, K., Ohshima, M., Piletska, E., 2013. Analyst 138, 5121-5128.

Zhou, Q., Li, E., Wang, Z., Gong, Y., Wang, C., Guo, L., Li, H., 2015. Journal of Breath Research 9, 016002.

Uzun, L., Turner, A.P.F., 2016. Biosensors and Bioelectronics 76, 131-144.

Research Highlights:

- C**onducting molecularly imprinted polymer biosensors** are synthesized and integrated with microfluidic biochips on a **handheld electronic analyzer. The developed system can detect propofol in human plasma samples within tens of seconds.**
- We have **systematically investigated the major parameters** that can affect the performance of the biosensors.
- Compared with the other methods, the proposed method is label-free, low-cost, and easy-to-use.
- A plastic biochip with our developed MIP biosensors is demonstrated.

Scheme 1. Schematic of the developed propofol sensing system based on the conduction of molecularly imprinted biosensors. (a) Handheld analyzer, (b) propofol capture and sensing on the molecularly imprinted biosensor, and (c) the specific binding of propofol molecules in imprinted nanocavities.

Scheme 2. Electrical equivalent circuit of a single conducting MIP electrode before and after propofol molecular binding.

Figure 1. Photographs of the fabricated propofol sensing system. (a) microfluidic stickers, (b) handheld system with plastic microfluidic chip, (c) plastic microfluidic biochip with on-chip conducting molecularly-imprinted biosensors, and (d) electropolyermized conducting molecularly-imprinted polymer on gold IDA electrodes.

Figure 2. Electropolymerization results. (a)–(d) SEM images and (e) electropolymerized MIP thickness including durations.

Figure 3. Dynamic measurements during analyte binding on MIP biosensors. (a) capacitance measurements and (b) resistance measurements.

Figure 4. Single-step propofol detection in human serum samples using the developed handheld analyzer. (a) Dynamic measurements of propofol obtained using NIP IDA electrodes (b) dynamic measurements of propofol obtained using conducting MIP IDA biosensors, (c) RC valve for different propofol concentrations, and (d) sensor-to-sensor variations for three propofol concentrations using the developed handheld analyzer.

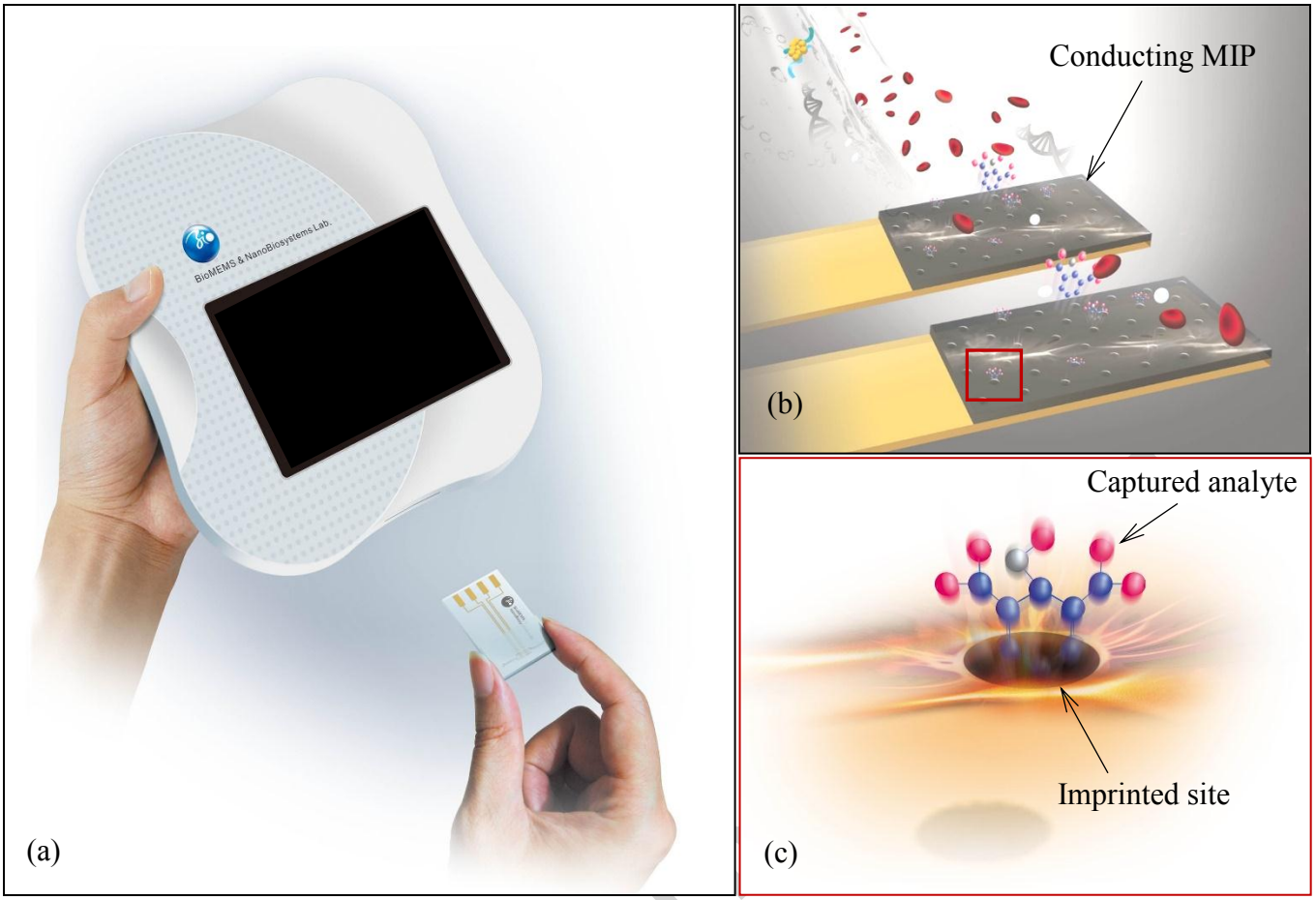

Scheme 1. Schematic of our developed propofol sensing system based on molecularly-imprinted biosensors. (a) handheld analyzer, (b) propofol capture and sensing on the molecularly imprinted biosensor, and (c) specific binding of propofol molecules in imprinted nanocavities.

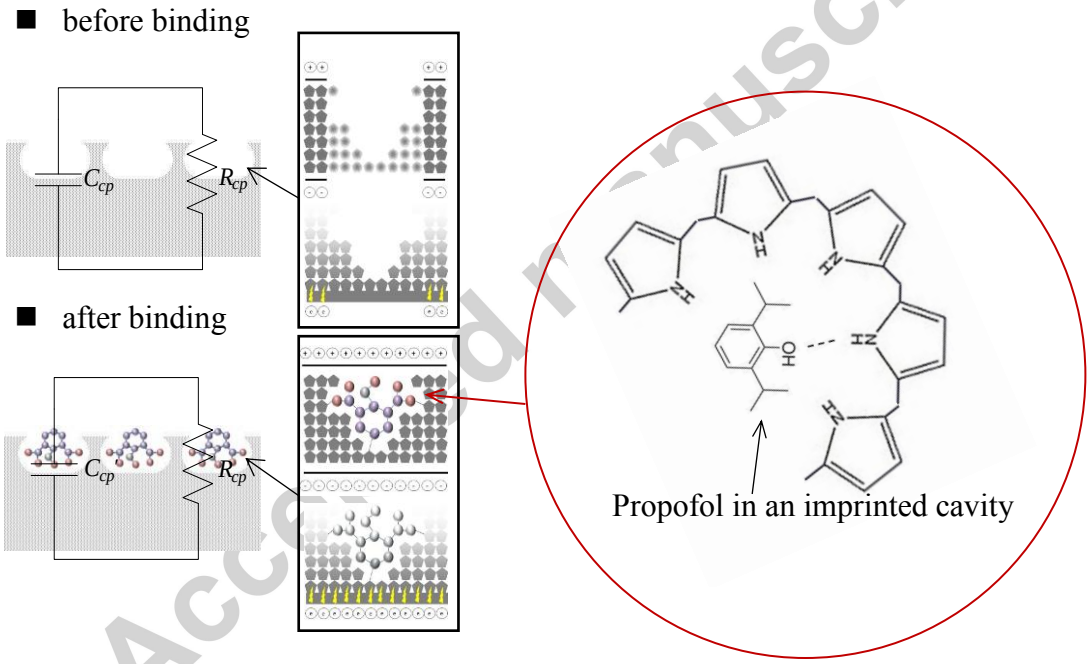

Scheme 2. Electrical equallivent circuit of the single conducting MIP electrode before and after propofol molecule binding.

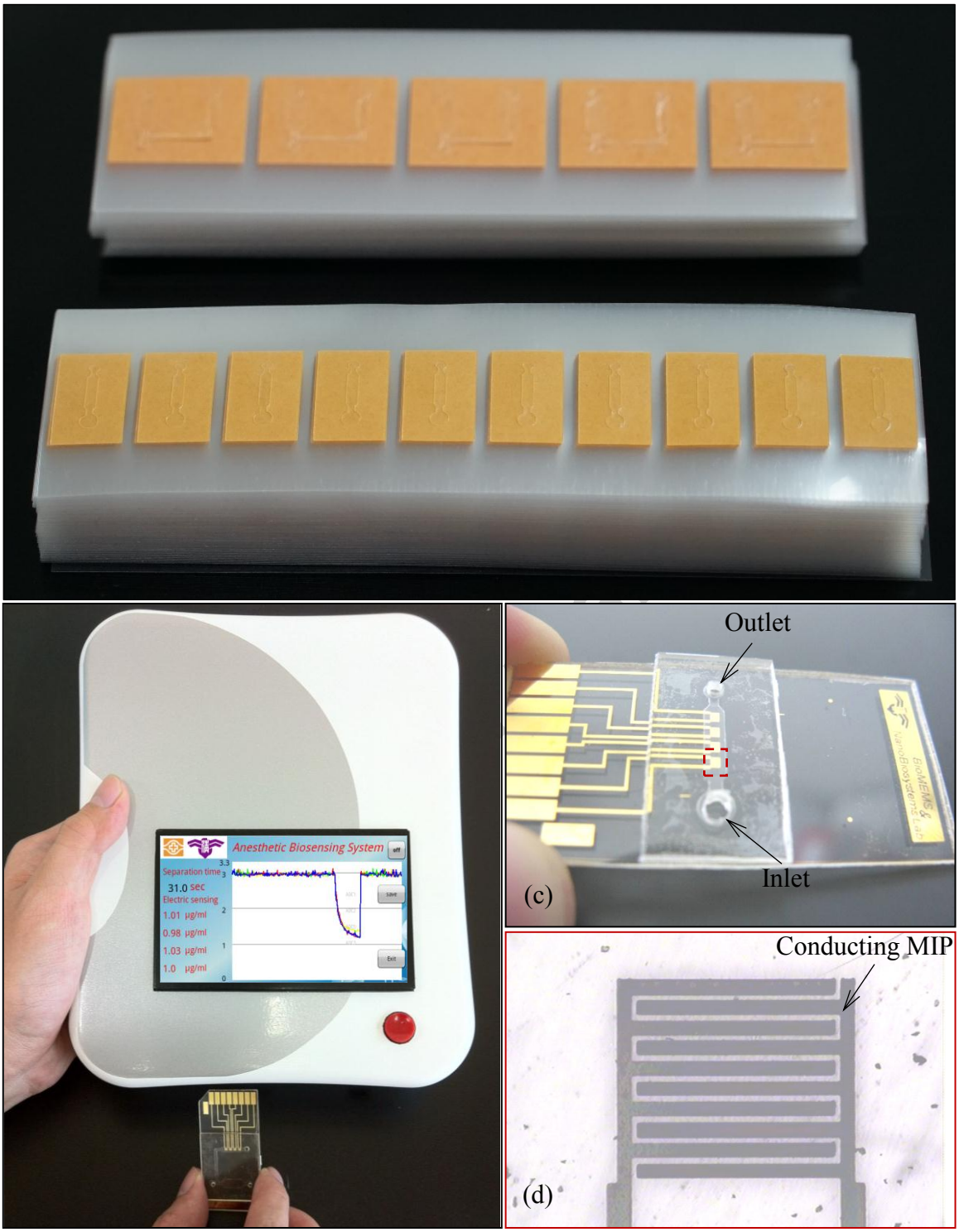

Figure 1. Photographs of the fabricated propofol sensing system. (a) microfluidic stickers, (b) handheld system with plastic microfluidic chip, (c) plastic microfluidic biochip with on-chip conducting molecularly-imprinted biosensors, and (d) electropolyermized conducting molecularly-imprinted polymer on gold IDA electrodes.

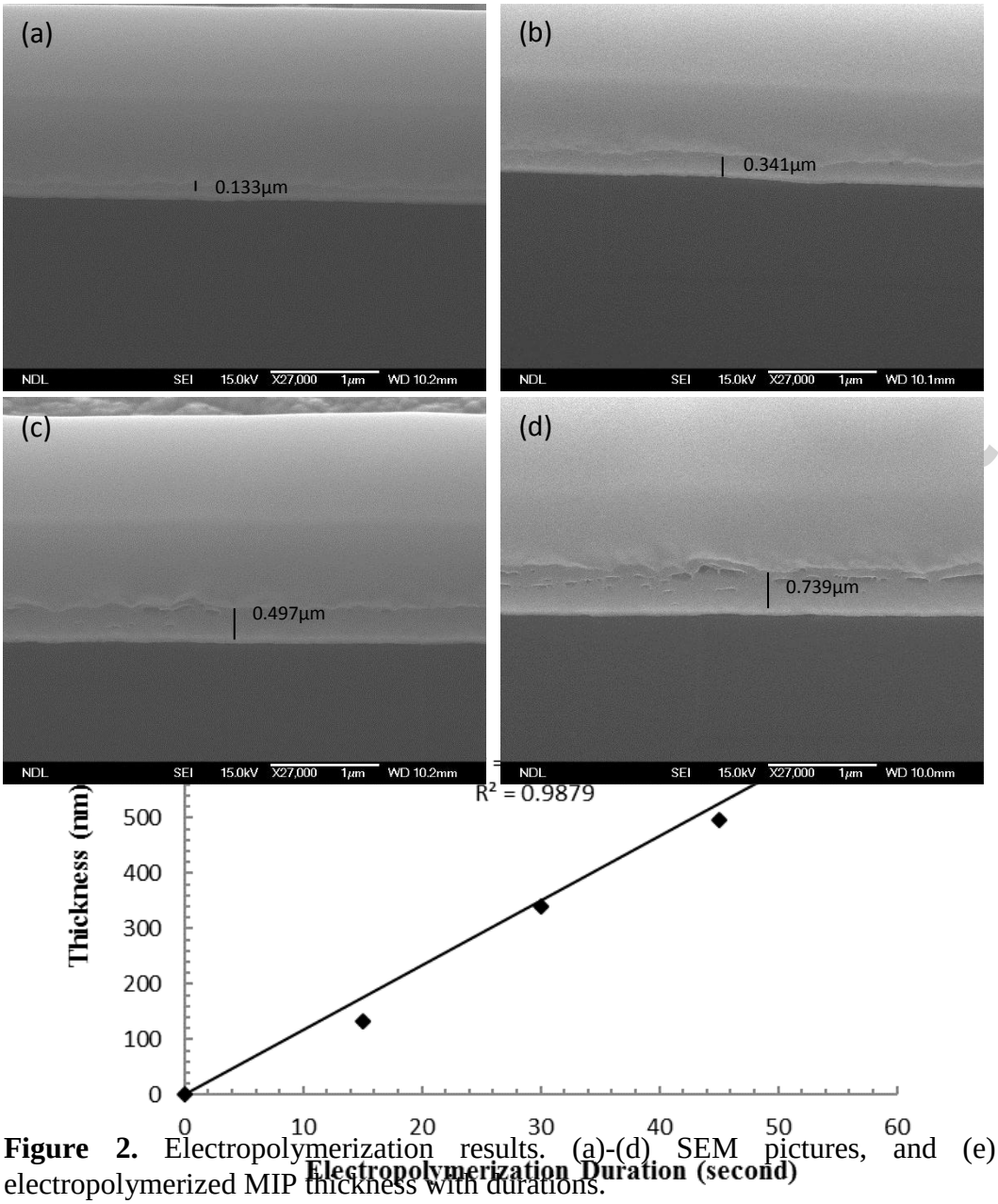

Figure 2. Electropolymerization results. (a)-(d) SEM pictures, and (e) electropolymerized MIP thickness with durations.

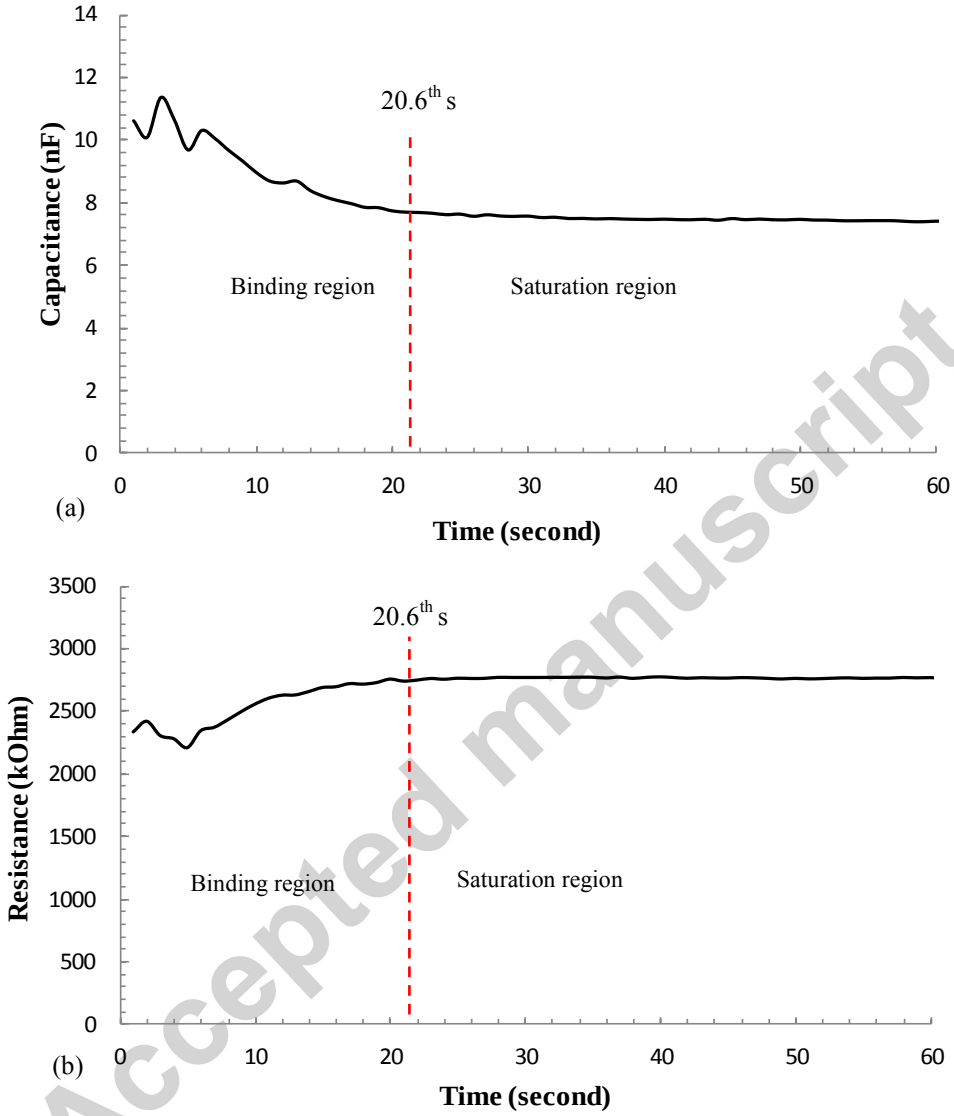

Figure 3. Dynamic measurements during analyte binding on MIP biosensors. (a) capacitance measurements and (b) resistance measurements.

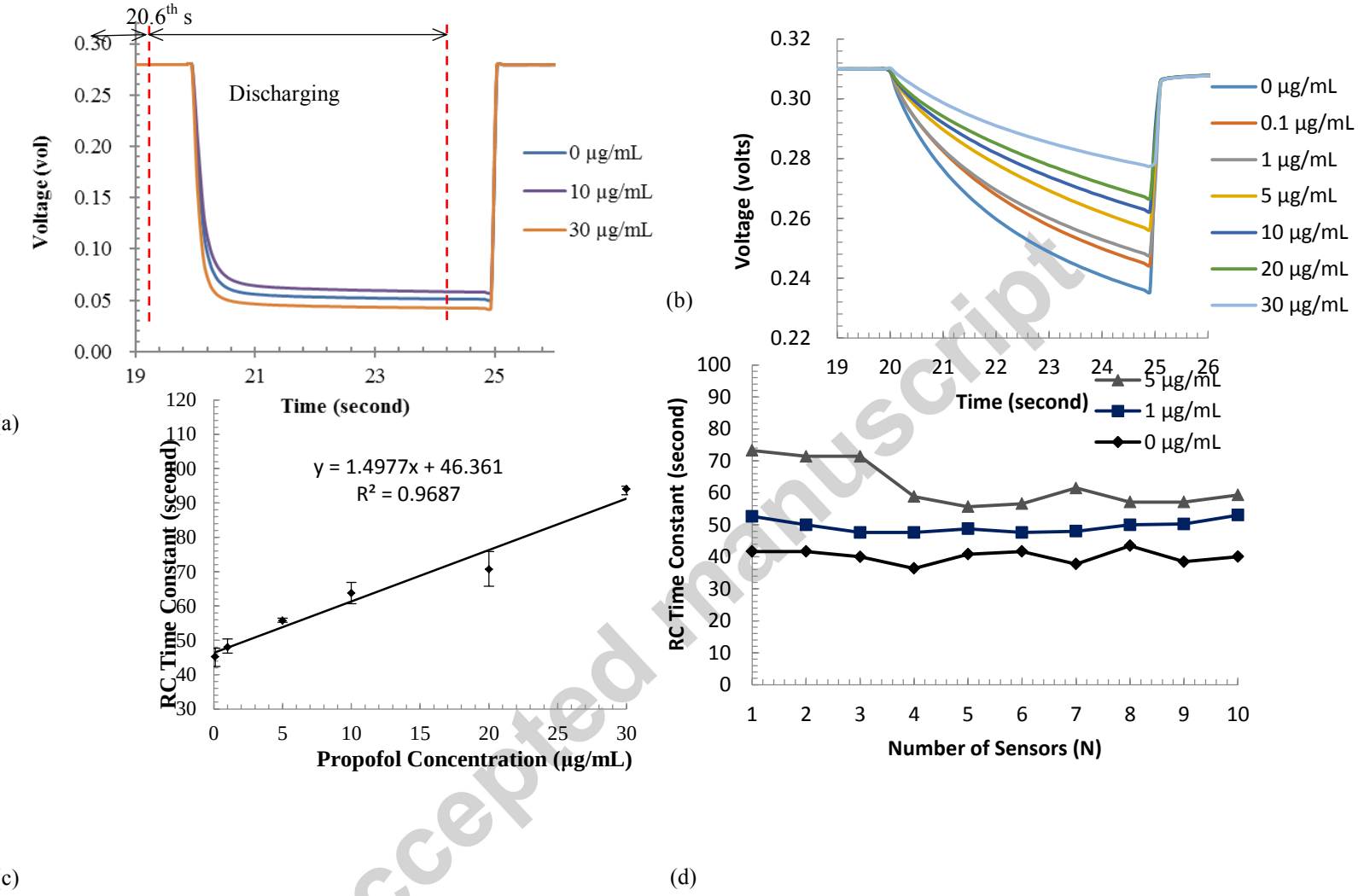

Figure 4. Single-step propofol detection in human serum samples by using the developed handheld analyzer. (a) dynamic measurements of propofol using NIP IDA electrodes, (b) dynamic measurements of propofol using conducting MIP IDA biosensors (c) RC value for different propofol concentrations as the calibration curve, and (d) sensor-to-sensor variation for three different propofol concentrations using the developed handheld analyzer.